Heterometallic Eu/M(II) Benzenethiolates (M = Zn, Cd, Hg): Synthesis, Structure, and Thermolysis Chemistry

Meggan Brewer, Jongseong Lee, and J. G. Brennan*

Department of Chemistry, Rutgers, The State University of New Jersey, Piscataway, New Jersey 08855-0939

Received May 19, 1995[⊗]

Europium–mercury amalgam reacts with diphenyl disulfide in THF to give a heterometallic product that crystallizes from pyridine (py) as $[(py)_3Eu(\mu_2\text{-}SPh)_2(\mu_3\text{-}SPh)Hg(SPh)]_2\cdot 2py$ (**1**). Cluster **1** reacts with Cd in pyridine to give $[(py)_3Eu(\mu_2\text{-}SPh)_2(\mu_3\text{-}SPh)Cd(SPh)]_2\cdot 2py$ (**2**) and with Zn in THF to give $[(THF)_3Eu(\mu_2\text{-}SPh)_2(\mu_3\text{-}SPh)Zn(SPh)]_2\cdot$ THF (**3**). All three compounds have been characterized by NMR, IR, and UV–visible spectroscopy and by single-crystal X-ray diffraction. The three are structurally related; **1** and **2** are isostructural tetrametallic clusters with μ_2 and μ_3 thiolate ligands connecting the 7-coordinate Eu(II) and tetrahedral group 12 metal ions. The lanthanide coordination sphere is saturated with three neutral pyridine donors, and the group 12 metal ion is bound to a terminal benzenethiolate ligand. The zinc cluster **3** has the same tetrametallic framework and connectivity as **1** and **2** but crystallizes in a different unit cell. The thermolysis products of these compounds have been established: **1** decomposes to give EuS, Ph_2S, Hg, and S_2Ph_2; **2** eliminates Ph_2S to give a mixture of CdS and EuS; **3** eliminates Ph_2S to give a mixture of EuS and ZnS. Crystal data for **1**–**3** (Mo Kα radiation, −100 °C): **1**, triclinic space group $\bar{P}1$, $a = 13.954(3)$ Å, $b = 15.311(4)$ Å, $c = 19.666(8)$ Å, $\alpha = 84.54(3)°$, $\beta = 86.40(3)°$, $\gamma = 87.25(3)°$, $Z = 2$; **2**, triclinic space group $\bar{P}1$, $a = 13.968(3)$ Å, $b = 15.387(6)$ Å, $c = 19.993(8)$ Å, $\alpha = 84.74(3)°$, $\beta = 86.21(3)°$, $\gamma = 87.30(3)°$, $Z = 2$; **3**, monoclinic space group $P2_1/n$, $a = 13.920(5)$ Å, $b = 17.049(5)$ Å, $c = 17.823(6)$ Å, $\beta = 103.7(3)°$, $Z = 4$.

Introduction

There are both fundamental and applied motivations for studying the coordination chemistry of lanthanide (Ln) elements bound to the softer chalcogens S, Se, and Te. Fundamentally, the nature of the bonding between these hard, ionic, electropositive metal ions and the soft, covalent chalcogens is relatively unexplored. While bonding in the solid state lanthanide chalcogenide compounds has long been discussed in terms of considerable covalent bonding character,[1] little is known about the nature of molecular Ln–chalcogen bonds.[2,3]

In the past few years there has been a surge of interest in preparing Ln complexes with chalcogenolates as the only anions.[3] This effort is inspired not only by the desire to understand molecular lanthanide–chalcogen bonding but also because of the potential use of Ln chalcogenolates as single-source dopants for the rapidly emerging fields of Ln-doped semiconductors[4a–l] and fiber optic materials based on the heavier chalcogens.[4m–s] A wide variety of chalcogenolate ligands, each imparting unique physical properties, have been used to stabilize divalent and trivalent lanthanide ions.

More recently, heterometallic Ln–group 12 metal benzeneselenolates have been isolated and structurally characterized.[5] These molecules are sterically uncongested derivatives of monometallic Ln chalcogenolates and, as such, can serve to enhance our understanding of the Ln–chalcogen bond. These molecules are also useful as models for understanding how the incorporation of an electropositive Ln ion into a covalent semiconductor lattice alters the physical properties of the covalent matrix. These heterometallic selenolates form a broad class of compounds in which Ln oxidation state, neutral donor ligands, the group 12 metal (M), and the Ln:M ratio are potential variables. The soft, covalent chalcogenolate ligands bound to hard, unpolarizable Ln ions are effectively stabilized by chelating the soft group 12 metal.

An extension of this chemistry to the synthesis of heterometallic Ln–M thiolates is of interest both because the scope and

[⊗] Abstract published in *Advance ACS Abstracts,* October 15, 1995.

(1) (a) Gerth, G.; Kienle, P.; Luchner, K. *Phys. Lett. A* **1968**, *27*, 557–8. (b) Eatough, N. L.; Hall, H. T. *Inorg. Chem.* **1970**, *9*, 417–8. (c) Dagys, R. S.; Anisimov, F. G. *Sov. Phys. Solid State* **1984**, *26*, 547–8. (d) Wachter, P. *Crit. Rev. Solid State* **1972**, *3*, 189–241. (e) Byrom, E.; Ellis, D. E.; Freeman, A. J. *Phys. Rev. B* **1976**, *14*, 3558–68. (f) Zhukov, V. P.; Gubanov, V. A.; Weber, J. *J. Chem. Phys. Solids* **1981**, *42*, 631–9.

(2) (a) Schumann, H.; Albrecht, I.; Hahn, E. *Angew. Chem., Int. Ed. Engl.* **1985**, *24*, 985–6. (b) Berg, D.; Burns, C.; Andersen, R. A.; Zalkin, A. *Organometallics* **1988**, *8*, 1858–63. (c) Berg, D. J.; Burns, C.; Andersen, R. A.; Zalkin, A. *Organometallics* **1989**, *8*, 1865–70. (d) Zalkin, A.; Berg, D. J. *Acta Crystallogr.* **1988**, *44C*, 1488–9. (e) Evans, W.; Grate, J. W.; Bloom, I.; Hunter, W. E.; Atwood, J. L. *J. Am. Chem. Soc.* **1985**, *107*, 405–9. (f) Evans, W.; Rabe, G.; Ziller, J.; Doedens, R. *Inorg. Chem.* **1994**, *33*, 2719–26. (g) Welder, M.; Noltemeyer, M.; Pieper, U.; Schmidt, H.; Stalke, D.; Edelmann, F. *Angew. Chem., Int. Ed. Engl.* **1990**, *29*, 894–6. (h) Evans, W.; Rabe, G. W.; Ansari, M. A.; Ziller, J. *Angew. Chem., Int. Ed. Engl.* **1994**, 33, 2110–1. (i) Wedler, M.; Recknagel, A.; Gilje, J. W.; Nottemeyer, M.; Edelmann, F. T. *J. Organomet. Chem.* **1992**, *426*, 295.

(3) (a) Cetinkaya, B.; Hitchcock, P. B.; Lappert, M. F.; Smith, R. G. *J. Chem. Soc., Chem. Commun.* **1992**, 932–3. (b) Strzelecki, A. R.; Timinski, P. A.; Hesel, B. A.; Bianconi, P. A. *J. Am. Chem. Soc.* **1992**, *114*, 3159–60. (c) Cary, D. R.; Arnold, J. *J. Am. Chem. Soc.* **1993**, *115*, 2520–1. (d) Berardini, M.; Emge, T.; Brennan, J. G. *J. Chem. Soc., Chem. Commun.* **1993**, 1537–8. (e) Berardini, M.; Emge, T.; Brennan, J. G. *J. Am. Chem. Soc.* **1993**, *115*, 8501–2. (f) Khasnis, D. V.; Lee, J.; Brewer, M.; Emge, T. J.; Brennan, J. G. *J. Am. Chem. Soc.* **1994**, *116*, 7129–33. (g) Brewer, M.; Khasnis, D.; Buretea, M.; Berardini, M.; Emge, T. J.; Brennan, J. G. *Inorg. Chem.* **1994**, *33*, 2743–7 (h) Carey, D. R.; Arnold, J. *Inorg. Chem.* **1994**, *33*, 1791–5. (i) Mashima, K.; Nakayama, Y.; Kanehisa, N.; Kai, Y.; Nakamura, A. *J. Chem. Soc., Chem. Commun.* **1993**, 1847–8. (j) Strzelecki, A. R.; Likar, C.; Hesel, B. A.; Utz, T.; Lin, M. C.; Bianconi, P. A. *Inorg. Chem.* **1994**, *33*, 5188–94. (k) Mashima, K.; Nakayama, Y.; Fukumoto, H.; Kanehisa, N.; Kai, Y.; Nakamura, A. *J. Chem. Soc., Chem. Commun.* **1994**, 2523–4. (l) Tatsumi, K.; Amemiya, T.; Kawaguchi, H.; Tani, K. *J. Chem. Soc., Chem. Commun.* **1993**, 773–4. (m) Lee, J.; Brewer, M.; Berardini, M.; Brennan, J. G. *Inorg. Chem.* **1995**, *34*, 3215. (n) Carey, D.; Ball, G. E.; Arnold, J. *J. Am. Chem. Soc.* **1995**, *117*, 3492. (o) Berardini, M.; Brennan, J. G. *Inorg. Chem.*, in press.

0020-1669/95/1334-5919$09.00/0

limitations of heterometallic chalcogenolate chemistry can be established and because the wider band gaps of the solid state group 12 sulfides make Ln-doped sulfide materials more likely candidates for optoelectronic device fabrication. This paper reports our initial results in Ln−group 12 metal thiolate chemistry. We show that hard and soft metal thiolates react to form stable heterometallic compounds. The effect of M on the Ln−S bond is discussed, and the identities of the solid state products that result from the thermal decomposition of these heterometallic compounds are established.

Experimental Section

General Procedures. All syntheses were carried out under ultrapure nitrogen (JWS), using conventional drybox or Schlenk techniques. Solvents (Fisher) were refluxed continuously over molten alkali metals or sodium/benzophenone, and collected immediately prior to use. Anhydrous pyridine (py) was purchased (Aldrich) and used as received. PhSSPh was purchased from Aldrich and recrystallized from hexane. Melting points were taken in sealed capillaries and are uncorrected. X-ray powder diffraction patterns were obtained on a SCINTAG PAD V diffractometer with Cu Kα radiation. IR spectra were taken using KBr plates with a Perkin Elmer 1720X FTIR at 4 cm^{-1} resolution from 4000 to 600 cm^{-1}. Electronic spectra were recorded on a Varian DMS 100S spectrometer with the samples in a 0.10 mm quartz cell attached to a Teflon stopcock. Elemental analyses were performed by Quantitative Technologies, Inc. (Salem, NJ).

$[(py)_3Eu(\mu_2\text{-}SPh)_2(\mu_3\text{-}SPh)Hg(SPh)]_2\cdot 2py$ (1). THF (60 mL) was added to a Schlenk tube containing diphenyl disulfide (1.42 g, 6.50 mmol), Hg (2.32 g, 11.60 mmol), and Eu (494 mg, 3.25 mmol). The reaction mixture turned bright yellow within 15 min, and a yellow solid formed within 2 h. The reaction mixture was stirred for 4 days and then taken to dryness under vacuum. The yellow solid was washed with hexane and then dissolved in pyridine (15 mL) to give a red solution. The solution was filtered, and orange crystals (2.43 g, 64%) were obtained by a slow diffusion of diethyl ether into the pyridine solution. The crystals desolvated at 50 °C, eliminated Hg at 130 °C, and decomposed at 390 °C. The uncoordinated pyridine diffused from the lattice within an hour of isolation. Anal. Calcd for $C_{39}H_{35}N_3S_4EuHg$: C, 45.6; H, 3.44; N, 4.09. Found: C, 46.0; H, 3.27; N, 4.73. IR: 2710 (w), 1560 (w), 1370 (s), 1290 (w), 1160 (w), 1140 (w), 715 (m) cm^{-1}. UV: λ_{max} (ca. 1 mg/mL of pyridine) = 303 nm; λ_{max} (ca. 1 mg/mL of THF) = 232, 272 nm. The ^1H NMR (ca. 10 mg/0.5 mL of THF-d_8) spectrum contained resonances at 8.55 (broad), 7.67 (triplet), and 7.26 (doublet) ppm that were too broad to integrate.

Thermolysis. 1 was placed in a Pyrex tube under vacuum for 1 h. The tube was then sealed, and the sample temperature was raised over a period of 3 days from 50 to 400 °C, with one end of the tube kept at room temperature. Between 80 and 100 °C, a colorless liquid (pyridine) condensed in the part of the tube that was kept outside the furnace (cold zone). Between 250 and 300 °C, brown diphenylsulfide, white crystalline diphenyl disulfide, and mercury condensed in the cold zone. The volatile materials were identified by ^1H NMR spectroscopy. The remaining black solid was transferred to a quartz tube that was then sealed under vacuum (10^{-7} Torr). Further heating (700 °C, 5 days) showed no further elimination of volatile products and an X-ray powder diffraction profile of the final solid product indicated that EuS[6] was the only crystalline phase present. The "yield" of the final product fluctuates with the initial size of the crystals used in the pyrolysis experiment, due to the variable rate at which the lattice pyridine is lost.

$[(py)_3Eu(\mu_2\text{-}SPh)_2(\mu_3\text{-}SPh)Cd(SPh)]_2\cdot 2py$ (2). Cd (4.02 g, 36.00 mmol) was added to a solution of **1** (2.43 g, 2.20 mmol) in pyridine (40 mL). The reaction mixture was stirred for 7 days at 90 °C and then concentrated to dryness, and the residue was washed with diethyl ether. The orange solid was redissolved in pyridine (30 mL), and the solution was filtered. Orange crystals (1.22 g, 55%) were obtained by slow diffusion of diethyl ether into the pyridine solution. The compound lost solvent and turned yellow at 120 °C, slowly turned orange, and then became dark red at 400 °C. The uncoordinated pyridine diffused from the lattice within an hour of isolation at room temperature. Anal. Calcd for $C_{39}H_{35}N_3S_4EuCd$: C, 49.9; H, 3.76; N, 4.47. Found: C, 48.8; H, 4.19; N, 4.64. IR: 2710 (w), 1560 (w), 1370 (s), 1290 (w), 1178 (w), 1155 (w), 715 (m) cm^{-1}. The ^1H NMR spectra (approximately 10 mg/0.5 mL of THF-d_8) contained broad resonances at 8.53, 7.65, and 7.25 (d) ppm. UV: λ_{max} (ca. 1 mg/mL of pyridine) = 298, 314 nm; λ_{max} (ca. 1 mg/mL of THF) = 212, 251 nm; λ_{max} (ca. 1 mg/mL of CH_3CN) = 208, 273 nm.

Thermolysis. 2 (1017 mg) was placed in a Pyrex tube under vacuum for 1 h. The tube was sealed, and the sample temperature was raised over a period of 5 days from 50 to 500 °C. At temperatures of 80−100 °C, a colorless liquid (pyridine) condensed in the cold zone, and at 250−300 °C, brown diphenylsulfide condensed. The volatile materials were identified by ^1H NMR spectroscopy. The remaining black solid (356 mg, 108%) was transferred to a quartz tube that was then sealed under vacuum (10^{-7} Torr). Further heating (700 °C, 5 days) showed no further elimination of volatile products, and the X-ray powder diffraction profile of the solid product contained peaks due to microcrystalline EuS and CdS.[7]

$[(THF)_3Eu(\mu_2\text{-}SPh)_2(\mu_3\text{-}SPh)Zn(SPh)]_2\cdot THF$ (3). Zinc (5.0 g, 76 mmol) was added to a solution of **1** (2.82 g, 1.04 mmol) in THF (50 mL), and the reaction mixture was stirred for 9 days at 65 °C. The solution was filtered while hot, and yellow crystals (0.52 g, 21%; mp 370 °C dec) were obtained upon cooling. Anal. Calcd for $C_{36}H_{44}O_3S_4EuZn$: C, 49.7; H, 5.11. Found: C, 48.9; H, 5.30. The ^1H NMR spectrum (ca. 10 mg/mL of CD_3CN) contained resonances at 8.34, 7.67, 7.21, 7.34, 3.66, and 1.79 ppm that were too broad ($w_{1/2}$ ca. 100 Hz) to integrate accurately. IR: 2724 (w), 1573 (w), 1461 (s), 1377 (s), 1304 (w), 1168 (w), 1081 (w), 1022 (w), 723 (m), 691 (w), 476 (w) cm^{-1}. UV: λ_{max} (ca. 3 mg/mL of pyridine) = 390 nm.

Thermolysis. In a fashion identical to that for the thermolysis of **2**, 520 mg of **3** was thermally converted into a black solid (150 mg, 97%), and X-ray powder diffraction indicated the presence of both microcrystalline EuS and ZnS.[8]

X-ray Crystallography of 1−3. Data for **1−3** were collected on a CAD4 diffractometer with graphite-monochromatized Mo Kα radiation (λ = 0.710 73 Å) at 153 K. In all structures, three check reflections were measured every 3 h and showed no significant intensity variation. The data were corrected for Lorentz effects and polarization. Absorp-

(4) (a) Pomrenke, G. S.; Klein, P. B.; Langer, D. W. *Rare Earth Doped Semiconductors*; MRS Symposium 301; Materials Research Society: Pittsburgh, PA, 1993. (b) Singer, K. E.; Rutter, P.; Praker, A. R.; Wright, A. C. *Appl. Phys. Lett.* **1994**, *64*, 707−9. (c) Swiatek, K.; Godlewski, M.; Niinisto, L.; Leskela, M. *J. Appl. Phys.* **1993**, *74*, 3442−6. (d) Taniguchi, M.; Takahei, K. *J. Appl. Phys* **1993**, *73*, 943−7. (e) Jourdan, N.; Yamaguchi, H.; Harikoshi, Y. *Jpn. J. Appl. Phys.* **1993**, *32*, 1784−7. (f) Kalboussi, A.; Moneger, S.; Marrakchi, G.; Guillot, G.; Lambert, B.; Guivarc'h, A. *J. Appl. Phys.* **1994**, *75*, 4171−5. (g) Takahei, K.; Taguchi, A.; Harikoshi, Y.; Nakata, J. *J. Appl. Phys.* **1994**, *76*, 4332−9. (h) Lozykowski, H. J.; Alshawa, A. K.; Brown, I. *J. Appl. Phys.* **1994**, *76*, 4836−46. (i) Kimura, T.; Isshiki, H.; Ishida, H.; Yugo, S.; Saito, R.; Ikoma, T. *J. Appl. Phys.* **1994**, *76*, 3714−9. (j) Charreire, Y.; Tolomen-Kivimaki, O.; Leskela, M.; Cortes, R.; Nykanen, E.; Soininen, P.; Niinisto, L. *Program and Abstracts of the ICFE-2, Aug 1−6, 1994*; Kansikas, J., Leslela, M., Eds.; University of Helsinki: Helsinki, Finland, 1994; p 326. (k) Charreire, Y.; Marbeuf, A.; Tourillon, G.; Leskela, M.; Niinisto, L.; Nykanen, E.; Soininen, P.; Tolonen, O. *J. Electrochem. Soc.* **1992**, *139*, 619−21. (l) Charreire, Y.; Svoronos, D. R.; Ascone, I.; Tolonen, O.; Niinisto, L.; Leskela, M. *J. Electrochem. Soc.* **1993**, *140*, 2015−9. (m) Kanamori, T.; Terunuma, Y.; Takahashi, S.; Miyashita, T. *J. Lightwave Technol.* **1984**, *LT2*, 607. (n) Kumta, P. N.; Risbud, S. H. *Am. Ceram. Soc. Bull.* **1990**, *69*, 1977. (o) Nishii, J.; Morimoto, S.; Yokota, R.; Yamagishi, T. *J. Non-Cryst. Solids* **1987**, *95/96*, 641−6. (p) Savage, J. A. *Infrared Optical Materials and Their Antireflection Coatings*; Adam Hilger Ltd.: British, U.K., 1985; pp 79−94. (q) Nishii, J.; Morimoto, S.; Inagawa, I.; Iizuka, R.; Yamashita, T.; Yokota, R.; Yamagishi, T. *J. Non-Cryst. Solids* **1992**, *140*, 199−208. (r) Sanghara, J. S.; Busse, L. E.; Aggarwall, I. D. *J. Appl. Phys.* **1994**, *75*, 4885−91. (s) Katsugama, T.; Matsumura, H. *J. Appl. Phys.* **1994**, *75*, 2743−8.

(5) (a) Berardini, M.; Emge, T. J.; Brennan, J. G. *J. Am. Chem. Soc.* **1994**, *116*, 6941−2. (b) Berardini, M.; Emge, T. J.; Brennan, J. G. *Inorg. Chem.* **1995**, *34*, 5327−34.

(6) JCPDS Diffraction Profile No. 26-1419.

(7) JCPDS Diffraction Profile No. 41-1049.

(8) JCPDS Diffraction Profile Nos. 36-1450 and 05-0566.

Table 1. Crystal Data and Structure Refinement Parameters for $[(py)_3Eu(\mu_2\text{-}SPh)_2(\mu_3\text{-}SPh)Hg(SPh)]_2\cdot 2py$ (**1**), $[(py)_3Eu(\mu_2\text{-}SPh)_2(\mu_3\text{-}SPh)Cd(SPh)]_2\cdot 2py$ (**2**), and $[(THF)_3Eu(\mu_2\text{-}SPh)_2(\mu_3\text{-}SPh)Zn(SPh)]_2\cdot THF$ (**3**)

	1	**2**	**3**
empirical formula	$C_{88}H_{80}Eu_2Hg_2N_8S_8$	$C_{88}H_{80}Eu_2Cd_2N_8S_8$	$C_{40}H_{52}EuO_4S_4Zn$
a (Å)	13.954(3)	13.968(3)	13.920(5)
b (Å)	15.311(4)	15.387(6)	17.049(5)
c (Å)	19.966(8)	19.993(8)	17.823(6)
α (deg)	84.54(3)	84.74(3)	90
β (deg)	86.40(3)	86.21(3)	103.70(3)
γ (deg)	87.25(3)	87.30(3)	90
V (Å^3)	4234(2)	4266(3)	4109(2)
Z	2	2	2
fw	2211.18	2034.80	942.39
space group	$P\bar{1}$ (No. 2)	$P\bar{1}$ (No. 2)	$P2_1/n$ (No.14)
temp (K)	−110	−110	−110
λ (Å)	0.710 73	0.710 73	0.710 73
D(calcd) (mg/m^3)	1.734	1.584	1.532
abs coeff (mm^{-1})	5.322	2.186	2.337
final $R(F_o)^a$ ($I > 2\sigma(I)$)	0.063	0.038	0.034
final $R_w(F_o^2)^a$ ($I > 2\sigma(I)$)	0.172	0.084	0.074

[a] Definitions: $R(F_o) = \sum||F_o| - |F_c||/\sum|F_o|$; $R_w(F_o^2) = \{\sum[w(F_o^2 - F_c^2)^2]/\sum[w(F_o^2)^2]\}^{1/2}$.

tion effects for **2** and **3** were corrected for by the empirical ψ-scan method. The structures were solved by direct methods (SHELXS86).[9] All non-hydrogen atoms were refined (SHELXL93)[10] on the basis of F_o^2. All hydrogen atom coordinates were calculated with idealized geometries (SHELXL93). Crystallographic data and final R indices are given in Table 1. Significant bond distances and angles for **1**−**3** are given in Tables 2−4, respectively. Tables of final significant atomic coordinates for **1**−**3** are given in Tables 5−7, respectively. Complete crystallographic details are given in the Supporting Information.

Results and Discussion

Synthesis and Structure. Europium−mercury amalgams reduce diphenyl disulfide cleanly in THF at room temperature to give a light yellow, slightly soluble product. Either the product can be dissolved in pyridine, or pyridine can be used as the reaction solvent. In either case, saturation of the pyridine solution with diethyl ether gives 60−70% yields of an orange crystalline compound. Spectroscopic and analytical characterization techniques provided little structural information on the product, due to the presence of the unpaired electrons on the Eu(II) (f^7) ion and the tendency of the product to desolvate at room temperature. For unambiguous structural determination, the compound was studied by low-temperature single-crystal X-ray diffraction and shown to be the heterotetrametallic benzenethiolate complex $[(py)_3Eu(\mu_2\text{-}SPh)_2(\mu_3\text{-}SPh)Hg(SPh)]_2$ (**1**). Table 2 gives a listing of significant bond geometries for **1**, and Figure 1 shows an ORTEP diagram of the complex. Compound **1** contains pairs of 7-coordinate Eu(II) ions and tetrahedral Hg(II) ions connected through a series of doubly and triply bridging benzenethiolate ligands. The Eu coordination sphere is saturated with three pyridine donors, and the Hg ion is bound to a terminal benzenethiolate ligand. The heavy-atom framework in **1** is structurally related to the tetrametallic selenolate clusters $[(L)_3Eu(\mu_2\text{-}SePh)_2(\mu_3\text{-}SePh)Hg(SePh)]_2$ (L = THF,[5a] py[5b]) as well as a series of tetrametallic group 12 metal thiolates.[11]

This tetrametallic chalcogenolate cluster framework appears to be particularly stable and in benzeneselenolate chemistry is found whenever the Ln−Se bond is relatively strong (i.e. Ln^{3+} rather than Ln^{2+}) or when the group 12 metal−chalcogen bonds are weak (i.e. Hg−Se rather than Zn−Se). It has been proposed that deviations from this tetrametallic structure occur when the relative bond strengths favor M−Se bonding, as, for example, in bimetallic $(THF)_4Eu(\mu\text{-}SePh)_3ZnSePh$ (**4**).[5b] In the structure of **4**, a combination of weak Ln(II)−Se bonds and stronger Zn−Se bonds results in the formation of a bimetallic complex containing three Eu−Se bonds rather than a tetrametallic structure with four Eu−Se bonds. In order to test the suggestion that the structure of **4** results from stronger Zn−Se bonding, we set out to isolate and characterize the Cd and Zn derivatives of **1** and establish the effect of M in a system with less polarizable chalcogenolate ligands.

The Hg in **1** can be replaced by the other group 12 metals. The reaction of **1** with elemental Cd in pyridine is slow and can take a period of days to weeks, depending on the surface area of the Cd used. Eventually, the reaction deposits elemental mercury, which can be identified visually. In order to establish the structural ramifications of this substitution, $[(pyridine)_3Eu(\mu_2\text{-}SPh)_2(\mu_3\text{-}SPh)Cd(SPh)]_2$ (**2**) was examined by low-temperature single-crystal X-ray diffraction. Tetrametallic **2** was found to be isostructural with **1**. Table 3 gives a listing of significant bond geometries for the complex, and an ORTEP diagram of **1** is given in Figure 1.

The Hg(II) ion can also be replaced with Zn(II). Attempts to crystallize the substitution product from pyridine were unsuccessful, but crystallization from THF gave $[(THF)_3Eu(\mu_2\text{-}SPh)_2(\mu_3\text{-}SPh)Zn(SPh)]_2$ (**3**) in 21% yield. Low-temperature single-crystal X-ray diffraction revealed that **3** has the same structural framework as **1** and **2**, although packing of the THF ligands leads to crystallization in a different space group. Table 4 gives a listing of significant bond geometries for **3**, and Figure

Table 2. Significant Bond Lengths (Å) and Angles (deg) for **1**

Hg(1)−S(1)	2.449(3)	Hg(1)−S(2)	2.523(3)	Hg(1)−S(4)	2.565(3)
Hg(1)−S(3)	2.683(3)	Hg(2)−S(5)	2.449(3)	Hg(2)−S(6)	2.535(3)
Hg(2)−S(8)	2.540(3)	Hg(2)−S(7)	2.694(3)		
Eu(1)−S(2)	3.050(3)	Eu(1)−S(6)	3.035(3)	Eu(1)−S(7)	3.034(3)
Eu(1)−S(3)	2.979(3)	Eu(2)−S(7)	3.059(3)	Eu(2)−S(8)	3.007(3)
Eu(2)−S(4)	3.017(3)	Eu(2)−S(3)	3.001(3)		
Eu(1)−N(1)	2.663(10)	Eu(1)−N(2)	2.717(10)	Eu(1)−N(3)	2.684(10)
Eu(2)−N(4)	2.689(10)	Eu(2)−N(5)	2.723(10)	Eu(2)−N(6)	2.655(10)

N(1)−Eu(1)−N(3)	73.5(3)	N(1)−Eu(1)−N(2)	143.4(3)
N(3)−Eu(1)−N(2)	72.7(3)	N(1)−Eu(1)−S(3)	131.3(2)
N(3)−Eu(1)−S(3)	147.9(2)	N(2)−Eu(1)−S(3)	77.1(2)
N(1)−Eu(1)−S(7)	74.5(2)	N(3)−Eu(1)−S(7)	146.1(2)
N(2)−Eu(1)−S(7)	140.9(2)	S(3)−Eu(1)−S(7)	65.39(8)
N(1)−Eu(1)−S(6)	120.3(2)	N(3)−Eu(1)−S(6)	107.7(2)
N(2)−Eu(1)−S(6)	83.3(2)	S(3)−Eu(1)−S(6)	78.89(9)
S(7)−Eu(1)−S(6)	79.44(9)	N(1)−Eu(1)−S(2)	82.4(2)
N(3)−Eu(1)−S(2)	92.9(2)	N(2)−Eu(1)−S(2)	85.7(2)
S(3)−Eu(1)−S(2)	74.11(9)	S(7)−Eu(1)−S(2)	93.74(9)
S(6)−Eu(1)−S(2)	152.52(8)	N(6)−Eu(2)−N(4)	71.6(3)
N(6)−Eu(2)−N(5)	70.5(3)	N(4)−Eu(2)−N(5)	141.8(3)
N(6)−Eu(2)−S(3)	148.7(2)	N(4)−Eu(2)−S(3)	77.0(2)
N(5)−Eu(2)−S(3)	140.6(2)	N(6)−Eu(2)−S(8)	89.8(2)
N(4)−Eu(2)−S(8)	96.7(2)	N(5)−Eu(2)−S(8)	78.3(2)
S(3)−Eu(2)−S(8)	93.36(9)	N(6)−Eu(2)−S(4)	105.1(2)
N(4)−Eu(2)−S(4)	99.7(2)	N(5)−Eu(2)−S(4)	94.8(2)
S(3)−Eu(2)−S(4)	80.51(9)	S(8)−Eu(2)−S(4)	160.63(8)
N(6)−Eu(2)−S(7)	146.0(2)	N(4)−Eu(2)−S(7)	141.1(2)
N(5)−Eu(2)−S(7)	75.8(2)	S(3)−Eu(2)−S(7)	64.81(8)
S(8)−Eu(2)−S(7)	79.17(9)	S(4)−Eu(2)−S(7)	81.61(9)
S(1)−Hg(1)−S(2)	120.85(10)	S(1)−Hg(1)−S(4)	118.09(11)
S(2)−Hg(1)−S(4)	112.69(10)	S(1)−Hg(1)−S(3)	113.74(11)
S(2)−Hg(1)−S(3)	88.48(10)	S(4)−Hg(1)−S(3)	95.63(10)
S(5)−Hg(2)−S(6)	119.06(12)	S(5)−Hg(2)−S(8)	118.79(12)
S(6)−Hg(2)−S(8)	113.83(10)	S(5)−Hg(2)−S(7)	107.64(11)
S(6)−Hg(2)−S(7)	95.69(10)	S(8)−Hg(2)−S(7)	95.17(10)

(9) Sheldrick, G. M. SHELXS86: Program for the Solution of Crystal Structures. University of Gottingen, Germany, 1986.
(10) Sheldrick, G. M. SHELXL93: Program for Crystal Structure Refinement. University of Gottingen, Germany, 1993.

Table 3. Significant Bond Lengths (Å) and Angles (deg) for **2**

Cd(1)−S(1)	2.461(3)	Cd(1)−S(2)	2.543(3)	Cd(1)−S(4)	2.544(3)
Cd(1)−S(3)	2.618(3)	Cd(2)−S(5)	2.467(3)	Cd(2)−S(8)	2.522(3)
Cd(2)−S(6)	2.573(3)	Cd(2)−S(7)	2.610(3)		
Eu(1)−S(2)	2.986(3)	Eu(1)−S(6)	3.024(3)	Eu(1)−S(7)	3.031(3)
Eu(1)−S(3)	3.081(3)	Eu(2)−S(7)	2.999(3)	Eu(2)−S(8)	3.039(3)
Eu(2)−S(4)	3.042(3)	Eu(2)−S(3)	3.073(3)		
Eu(1)−N(1)	2.713(8)	Eu(1)−N(2)	2.697(9)	Eu(1)−N(3)	2.661(9)
Eu(2)−N(4)	2.666(9)	Eu(2)−N(5)	2.699(8)	Eu(2)−N(6)	2.672(8)
N(3)−Eu(1)−N(2)	70.3(3)	N(3)−Eu(1)−N(1)	72.2(3)		
N(2)−Eu(1)−N(1)	142.1(3)	N(3)−Eu(1)−S(2)	91.4(2)		
N(2)−Eu(1)−S(2)	79.8(2)	N(1)−Eu(1)−S(2)	95.8(2)		
N(3)−Eu(1)−S(6)	105.2(2)	N(2)−Eu(1)−S(6)	94.8(2)		
N(1)−Eu(1)−S(6)	100.1(2)	S(2)−Eu(1)−S(6)	159.84(8)		
N(3)−Eu(1)−S(7)	149.3(2)	N(2)−Eu(1)−S(7)	140.2(2)		
N(1)−Eu(1)−S(7)	77.2(2)	S(2)−Eu(1)−S(7)	91.85(8)		
S(6)−Eu(1)−S(7)	79.80(8)	N(3)−Eu(1)−S(3)	145.9(2)		
N(2)−Eu(1)−S(3)	75.9(2)	N(1)−Eu(1)−S(3)	140.6(2)		
S(2)−Eu(1)−S(3)	78.36(8)	S(6)−Eu(1)−S(3)	81.49(8)		
S(7)−Eu(1)−S(3)	64.27(7)	N(4)−Eu(2)−N(6)	73.2(3)		
N(4)−Eu(2)−N(5)	143.2(3)	N(6)−Eu(2)−N(5)	73.0(3)		
N(4)−Eu(2)−S(7)	131.7(2)	N(6)−Eu(2)−S(7)	148.7(2)		
N(5)−Eu(2)−S(7)	77.2(2)	N(4)−Eu(2)−S(8)	83.2(2)		
N(6)−Eu(2)−S(8)	93.3(2)	N(5)−Eu(2)−S(8)	84.9(2)		
S(7)−Eu(2)−S(8)	74.52(8)	N(4)−Eu(2)−S(4)	118.6(2)		
N(6)−Eu(2)−S(4)	107.0(2)	N(5)−Eu(2)−S(4)	84.9(2)		
S(7)−Eu(2)−S(4)	79.29(8)	S(8)−Eu(2)−S(4)	153.41(7)		
N(4)−Eu(2)−S(3)	74.8(2)	N(6)−Eu(2)−S(3)	146.1(2)		
N(5)−Eu(2)−S(3)	140.7(2)	S(7)−Eu(2)−S(3)	64.73(7)		
S(8)−Eu(2)−S(3)	93.63(8)	S(4)−Eu(2)−S(3)	79.11(7)		
S(1)−Cd(1)−S(2)	117.9(1)	S(1)−Cd(1)−S(4)	117.8(1)		
S(2)−Cd(1)−S(4)	113.60(9)	S(1)−Cd(1)−S(3)	108.7(1)		
S(2)−Cd(1)−S(3)	95.92(9)	S(4)−Cd(1)−S(3)	97.94(9)		
S(5)−Cd(2)−S(8)	119.4(1)	S(5)−Cd(2)−S(6)	116.3(1)		
S(8)−Cd(2)−S(6)	113.46(9)	S(5)−Cd(2)−S(7)	114.5(1)		
S(8)−Cd(2)−S(7)	90.85(9)	S(6)−Cd(2)−S(7)	97.05(9)		

Table 4. Significant Bond Lengths (Å) and Angles (deg) for **3**

Eu(1)−S(1)	2.986(2)	Eu(1)−O(2)	2.553(4)
Eu(1)−S(2)	3.074(2)	Eu(1)−O(3)	2.563(4)
Eu(1)−S(3)	2.989(2)	Eu(1)−O(1)	2.588(4)
Eu(1)−S(2)′	3.030(2)	Zn(1)−S(4)	2.288(2)
Zn(1)−S(3)	2.341(2)	Zn(1)−S(1)′	2.368(2)
Zn(1)−S(2)	2.424(2)		
O(2)−Eu(1)−O(3)	72.0(2)	O(2)−Eu(1)−O(1)	71.9(2)
O(3)−Eu(1)−O(1)	142.23(14)	O(2)−Eu(1)−S(1)	106.05(12)
O(3)−Eu(1)−S(1)	89.43(11)	O(1)−Eu(1)−S(1)	110.98(11)
O(2)−Eu(1)−S(3)	98.56(12)	O(3)−Eu(1)−S(3)	84.67(11)
O(1)−Eu(1)−S(3)	89.97(11)	S(1)−Eu(1)−S(3)	151.52(4)
O(2)−Eu(1)−S(2)′	147.89(11)	O(3)−Eu(1)−S(2)′	139.46(10)
O(1)−Eu(1)−S(2)′	77.97(10)	S(1)−Eu(1)−S(2)′	74.50(5)
S(3)−Eu(1)−S(2)′	92.19(5)	O(2)−Eu(1)−S(2)	144.72(11)
O(3)−Eu(1)−S(2)	73.98(11)	O(1)−Eu(1)−S(2)	137.84(11)
S(1)−Eu(1)−S(2)	82.57(5)	S(3)−Eu(1)−S(2)	69.01(5)
S(2)′−Eu(1)−S(2)	67.28(5)		
S(4)−Zn(1)−S(3)	117.53(7)	S(4)−Zn(1)−S(1)′	113.71(7)
S(3)−Zn(1)−S(1)′	110.01(6)	S(4)−Zn(1)−S(2)	121.35(7)
S(3)−Zn(1)−S(2)	92.26(6)	S(1)′−Zn(1)−S(2)	98.90(6)

2 gives an ORTEP diagram of the complex. Again, the Eu ion in **3** is 7-coordinate, with three neutral THF donors filling the Eu(II) coordination sphere. This contrasts with the structure of heterometallic benzeneselenolate $(THF)_4Eu(\mu_2\text{-}SePh)_3ZnSePh$, which has only three Eu−chalcogen bonds. The difference in structure can be related to the differences in size and electronegativity of the benzenechalcogenolates. The smaller, more electronegative thiolate forms stronger bonds to the lanthanide ion than does selenolate, and so while Zn is sufficiently polarizing to reduce the number of Eu−Se bonds, it is less effective in polarizing thiolate electron density away from the Eu(II) ion. Thus, a tetrametallic benzenethiolate structure is observed.

Table 5. Atomic Coordinates ($\times 10^4$) and Equivalent Isotropic Displacement Parameters ($Å^2 \times 10^3$) for the Significant Atoms in **1**

	x	*y*	*z*	*U*(eq)[a]
Hg(1)	4112(1)	−3982(1)	−2654(1)	22(1)
Hg(2)	1069(1)	−740(1)	−2360(1)	21(1)
Eu(1)	3197(1)	−2059(1)	−1328(1)	17(1)
Eu(2)	1923(1)	−2675(1)	−3561(1)	19(1)
S(1)	5582(2)	−4359(2)	−3320(2)	28(1)
S(2)	4133(2)	−3892(2)	−1400(2)	23(1)
S(3)	3598(2)	−2266(2)	−2788(1)	18(1)
S(4)	2515(2)	−4510(2)	−3004(2)	23(1)
S(5)	-458(3)	−365(3)	−1761(2)	40(1)
S(6)	2617(2)	−240(2)	−1949(2)	22(1)
S(7)	1460(2)	−2469(2)	−2064(1)	18(1)
S(8)	1105(2)	−818(2)	−3627(2)	23(1)

[a] $U_{(eq)}$ is defined as one-third of the trace of the orthogonalized $\mathbf{U}_{ij}$ tensor.

Table 6. Atomic Coordinates ($\times 10^4$) and Equivalent Isotropic Displacement Parameters ($Å^2 \times 10^3$) for the Significant Atoms in **2**

	x	*y*	*z*	*U*(eq)[a]
Eu(1)	3085(1)	2693(1)	8579(1)	22(1)
Eu(2)	1786(1)	2063(1)	6328(1)	20(1)
Cd(1)	3905(1)	798(1)	7353(1)	22(1)
Cd(2)	905(1)	3937(1)	7652(1)	23(1)
S(1)	5446(2)	389(2)	6771(2)	41(1)
S(2)	3855(2)	847(2)	8623(1)	27(1)
S(3)	3543(2)	2472(2)	7074(1)	20(1)
S(4)	2381(2)	249(2)	6936(1)	23(1)
S(5)	-579(2)	4348(2)	8308(1)	31(1)
S(6)	2474(2)	4510(2)	8016(1)	26(1)
S(7)	1401(2)	2278(2)	7798(1)	21(1)
S(8)	871(2)	3887(2)	6396(1)	27(1)

[a] *U*(eq) is defined as one-third of the trace of the orthogonalized $\mathbf{U}_{ij}$ tensor.

Table 7. Atomic Coordinates ($\times 10^4$) and Equivalent Isotropic Displacement Parameters ($Å^2 \times 10^3$) for the Significant Atoms in **3**

	x	*y*	*z*	*U*(eq)[a]
Eu(1)	1342(1)	6022(1)	5049(1)	23(1)
Zn(1)	1186(1)	3700(1)	4375(1)	25(1)
S(2)	12(1)	4771(1)	4079(1)	23(1)
S(1)	−526(1)	6955(1)	4687(1)	27(1)
S(3)	2465(1)	4539(1)	4981(1)	29(1)
S(4)	1473(1)	2892(1)	3427(1)	33(1)

[a] *U*(eq) is defined as one-third of the trace of the orthogonalized $\mathbf{U}_{ij}$ tensor.

The tetrametallic structure of **3** suggests that Ln−S bonds are not readily distorted, and this is confirmed by examining the bond geometries of **1**−**3**, which afford an excellent opportunity for establishing the overall structural influence of the group 12 metal on Ln−S bonds. Comparison of the Eu−S bond lengths in **1**−**3** shows that the group II metal does not significantly perturb the lanthanide−sulfur bonds. The average μ_2 Eu−S bond lengths (3.027(3) Å in **1**, 3.023(3) Å in **2**, and 2.988(2) Å in **3**) increase slightly as the group II metal changes from Hg to Cd to Zn, while the average μ_3 Eu−S bond lengths (3.019(3) Å in **1**, 3.046(3) Å in **2**, and 3.052(2) Å in **3**) show the opposite trend. In either case, the differences are minor, indicating that the Eu−S bond is not easily distorted. Again, this contrasts with heterometallic benzeneselenolate chemistry, where the weaker Ln−Se bonds are significantly distorted upon coordination of group 12 metals; i.e., the Eu−Se bonds in **4** are 0.08 Å longer than the doubly bridging Eu−Se bonds in $[(THF)_3EuHg(SePh)_4]_2$.[5a]

The M−S bond lengths in **1**−**3** can be compared with previously reported M−S bond lengths to determine how the Eu(II) ion influences the M−S bond. Neutral polymetallic Zn

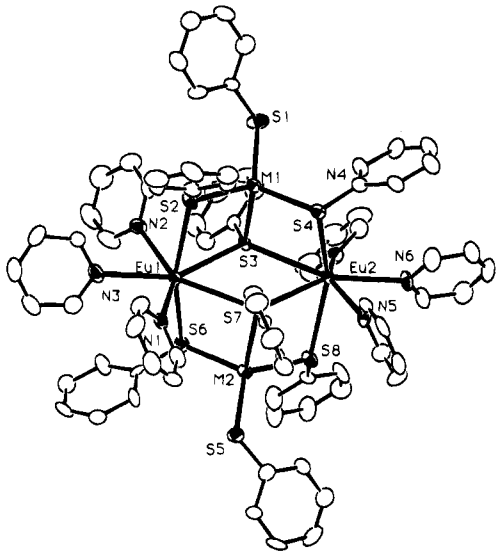

Figure 1. Molecular structures of $[(py)_3Eu(\mu_2\text{-}SPh)_2(\mu_3\text{-}SPh)M(SPh)]_2 \cdot 2$ py (compound **1**, M = Hg; compound **2**, M = Cd). The tetrametallic clusters contain 7-coordinate Eu ions and 4-coordinate group II metal ions, connected by μ_2 and μ_3 benzenethiolate ligands. The lattice pyridine has been omitted for clarity. Thermal ellipsoids (ORTEP) are drawn at the 50% probability level (M = Cd).

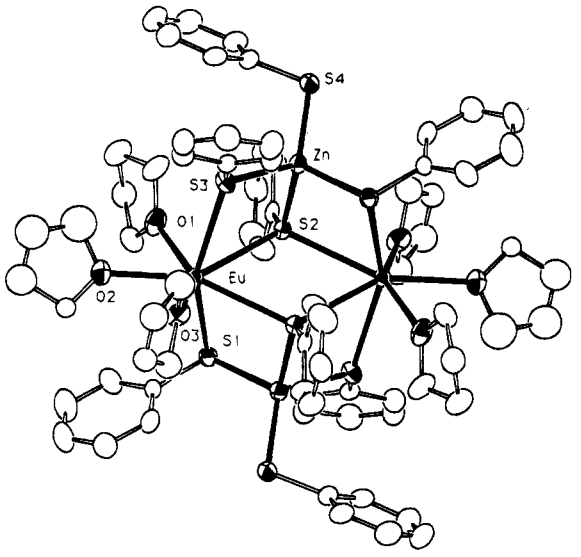

Figure 2. Molecular structure of $[(THF)_3Eu(\mu_2\text{-}SPh)_2(\mu_3\text{-}SPh)Zn(SPh)]_2 \cdot THF$. Tetrametallic cluster **3** has the same heavy-atom connectivity as **1** and **2** but is not isostructural. The lattice THF has been omitted for clarity. Thermal ellipsoids (ORTEP) are drawn at the 50% probability level.

and Cd benzenethiolates, as well as the adamantanoid dianion $Zn_4(SPh)_{10}^{2-}$, are most suitable reference points because they have phenyl substituents and are 4-coordinate group 12 metals; the structurally similar Zn and Cd tetrametallic thiolate halides[11] are less suitable because, in addition to the two M−S and two M−N bonds, the metals also interact to some extent with the halide ligands. If we compare the doubly bridging Cd−S bond lengths in **2** (2.546(3) Å) with the μ_2 Cd−S bond lengths in neutral $[Cd(SPh)_2]_n$ (2.54(1) Å),[12] we can determine that the presence of a Eu(II) ion does not significantly influence the length of a Cd−S bond. Zinc−sulfur bond lengths compare similarly. The average μ_2 Zn−S bond lengths in **3** (2.36(2) Å) are statistically indistinguishable from the μ_2 Zn−S bond lengths in the $Zn_4(SPh)_{10}$ dianion (2.36(2) Å)[13] and a neutral $Zn(SPh)_2$ derivative[14] (2.35(2) Å).

UV−Visible Characterization. The UV−visible spectroscopic properties of the divalent lanthanide chalcogenolates in pyridine solution are dominated by intense metal-to-ligand charge transfer (MLCT) excitations that were assigned by comparison of visible properties of THF and pyridine derivatives and by comparison of isostructural $(py)_5Yb(TePh)_2$ and $(py)_5Eu(TePh)_2$.[3e-g] These transitions appear to be a sensitive indicator of the electron density at the lanthanide center. In heterometallic benzeneselenolate chemistry, coordination of $Eu(SePh)_2$ to $Hg(SePh)_2$ resulted in a higher Eu to py CT energy relative to the monometallic $Eu(SePh)_2$, and the CT energy was further increased by substitution of Zn for the Hg ion. This trend was interpreted in terms of the group 12 metals polarizing selenolate electron density away from the Eu ion.[5]

In contrast, in the present work there is no linear change in optical excitation energy as a function of group II metal in complexes **1**−**3**. Substitution of Cd for Hg does increase the energy required to transfer an electron from Eu to py, as might be expected since the Cd−S bonds will be stronger than Hg−S bonds. However, a continuation of this effect is not observed upon incorporation of Zn, and instead, complex **3** exhibits the lowest Eu−py CT energy of the three thiolates.

A determination of the heterometallic solution structure would be required for an unambiguous assessment of these anomalous MLCT energies. Our inability to isolate a heterometallic Eu/Zn complex from pyridine suggests that a nontetrametallic structure may exist for **3** in pyridine, and this complicates a direct comparison of spectroscopic data. In related heterometallic benzeneselenolate work, the dependence of solution structure on solvent has been well documented with studies on the hexametallic chalcogenolate complex $[Yb(THF)_6][Hg_5(SePh)_{12}]$.[5b] This complex cation−anion pair is indefinitely stable in THF solution, but when the compound is dissolved in acetonitrile, crystalline $Hg(SePh)_2$ precipitates over a period of days. More striking is the reaction of this $YbHg_5(SePh)_{12}$ salt with pyridine to give a Yb(III) heterometallic selenolate complex and elemental Hg. The dependence of solution structure upon the identity of the solvent precludes an assessment of the UV−visible data for **1**−**3**.

Thermolysis. The thermolysis chemistry of compounds **1**−**3** was investigated, and the final solid state thermolysis products were identified by X-ray powder diffraction. The Hg complex **1** decomposes by first eliminating Hg and PhSSPh, which can be identified visually. The remaining "$Eu(SPh)_2$" decomposes at elevated temperatures to eliminate Ph_2S, and X-ray powder diffraction was used to identify the remaining black solid as EuS. The formation of carbide impurities in the final product can be kept below 1% by slowly raising the oven temperature over a period of days. Rapid heating gives a black solid that has an identical XRPD profile, but with a significant amount (>8%) of carbide contamination that can be detected by combustion analysis. The separation of the component metals in the decomposition of **1** is not surprising—$Hg(SR)_2$ compounds have been shown either to reductively eliminate RSSR or to form HgS and R_2S, with the final product depending on the identity of R.[15] In the thermolysis of **1**, facile reductive

(11) (a) Fawcett, T. G.; Ou, C.-C.; Potenza, J. A.; Schugar, H. J. *J. Am. Chem. Soc.* **1978**, *100*, 2058−62. (b) Canty, A. J.; Raston, C. L.; White, A. H. *Aust. J. Chem.* **1978**, *31*, 677. (c) Hu, W. J.; Barton, D.; Lippard, S. J. *J. Am. Chem. Soc.* **1973**, *95*, 1170−3.

(12) Craig, D.; Dance, I. G.; Garbutt, R. *Angew. Chem., Int. Ed. Engl.* **1986**, *25*, 165.

(13) Hencher, J. L.; Khan, M. A.; Said, F. F.; Tuck, D. G. *Polyhedron* **1985**, *4*, 1263.

(14) Dance, I. *J. Am. Chem. Soc.* **1980**, *102*, 3445.

elimination produces two volatile products at temperatures considerably lower than the decomposition temperature of the residual "$Eu(SPh)_2$".

In contrast, the Cd complex **2** does not eliminate diphenyl disulfide and Cd. Instead, the only volatile product in the thermolysis reaction is Ph_2S, which collects in the cold part of the reaction tube. An XRPD profile of the final black thermolysis product indicates the presence of both CdS and EuS solids. The final solid state products are dependent on thermolysis conditions. Thermolysis of the Zn complex **3** also gives Ph_2S, and X-ray powder diffraction of the final solid state product again shows that phase separation has occurred to give ZnS and EuS.

These phase separations are important in defining the limits at which heterometallic precursors can be used to deliver ternary chalcogenide solids. Presumably phase separation results when the incommensurate lattices cannot accommodate what would be a 50% substitution of one metal in the lattice of another, and the relatively high concentrations of both metals ensure that there are sufficiently high concentrations of the metal chalcogenides to function as nucleation sites for the individual lattices.

(15) (a) Claeson, P. *J. Prakt. Chem.* **1877**, *15*, 193. (b) Kearn, R. *J. Am. Chem. Soc.* **1953**, *75*, 1865. (c) Peach, M. *J. Inorg. Nucl. Chem.* **1973**, *35*, 1046.

Conclusion

Heterometallic chalcogenolate chemistry has been extended to compounds containing thiolate ligands. Europium−mercury benzenethiolates can be prepared in high yield via the reduction of diphenyl disulfide with Eu−Hg amalgam in either THF or pyridine. The Hg can be substituted by transmetalation with either Cd or Zn. All three group II metal derivatives crystallize as tetrametallic clusters containing 7-coordinate Eu(II) ions and 4-coordinate group 12 metals in distorted tetrahedral geometries. An analysis of cluster M−S bond lengths indicates that the Eu−S bonds are not significantly perturbed by coordination to the softer metal ions. Thermal decomposition of these heterometallic compounds leads to phase separation of the component metal sulfides.

Acknowledgment. This work was supported by the National Science Foundation under Grant No. CHE-9204160.

Supporting Information Available: Tables of additional crystal and refinement data, bond geometries, and atomic and thermal parameters, fully labeled ORTEP diagrams, and X-ray powder diffraction patterns for the thermolysis products of **1**−**3** (30 pages). Ordering information is given on any current masthead page.

IC950608M